Synthesis, characterization and X-ray crystal structures of cyclam derivatives. Part IV. 1,4,8,11-Tetraazacyclotetradecane-5,12-dione and its diprotonated forms†

Laurent Frémond,[a] Enrique Espinosa,[a] Michel Meyer,[a] Franck Denat,[a] Roger Guilard,*[a] Volker Huch[b] and Michael Veith[b]

[a] *Laboratoire d'Ingénierie Moléculaire pour la Séparation et les Applications des Gaz (LIMSAG, CNRS UMR 5633), Faculté des Sciences, Université de Bourgogne, 6 boulevard Gabriel, 21100 Dijon, France. E-mail: Roger.Guilard@u-bourgogne.fr; Fax: +33 3 80 39 61 18; Phone: +33 3 80 39 61 11*

[b] *Anorganische Chemie, Universität des Saarlandes, 66041 Saarbrücken, Germany*

Received (in Strasbourg, France) 23rd June 2000, Accepted 11th September 2000
First published as an Advance Article on the web 15th November 2000

The synthesis, spectroscopic characterization (NMR, IR, MS) and protonation constants of a dioxocyclam derivative, 1,4,8,11-tetraazacyclotetradecane-5,12-dione (**1**), are described. The crystal structures of the free-base macrocycle and two diprotonated forms, with bromide and perchlorate as counter ions, have been determined by X-ray diffraction studies in order to evaluate the influence of both the secondary amine's protonation state and of the intermolecular hydrogen-bonding interactions on the macrocycle conformation. The spectroscopic, potentiometric and structural data indicate that both secondary amines behave independently from each other, their protonation inducing only limited conformational changes of the macrocyclic framework. In the crystal, the diprotonated species adopt two different [3,4,3,4] diamond-lattice-type conformations as a consequence of intermolecular hydrogen bonds involving the oxo groups and the surrounding anions.

The replacement of amine by amide groups in polyazacycloalkanes yields a series of ligands that are structural intermediates between the corresponding saturated macrocyclic polyamines and oligopeptides. 1,4,8,11-Tetraazacyclotetradecane-5,7-dione (**2**), also called *cis*-dioxocyclam (Scheme 1), and its N- or C-substituted derivatives have been among the most extensively studied macrocyclic oxopolyamines.[2] Originally, this compound was synthesized by Tabushi *et al.*;[3] the first complexes were studied two years later by Kodama and co-workers.[4,5] The main characteristic of this series of ligands is their ability to form neutral complexes with certain transition metal cations (*i.e.* Ni^{2+}, Cu^{2+}, Co^{2+} and Pd^{2+}) by displacing the amide proton.[6] In general, these dioxotetraamines are more selective towards metal ions and their complexes show faster dissociation kinetics when compared to the analogous cyclic tetraamines.[2] Their ligand fields are stronger and consequently these oxoamines may stabilize the less-common +3 oxidation state of copper or nickel, similarly to oligopeptides.[7] Appending additional chelating arms to the dioxotetraamine causes considerable changes in the coordination properties of the ligands.[8–11]

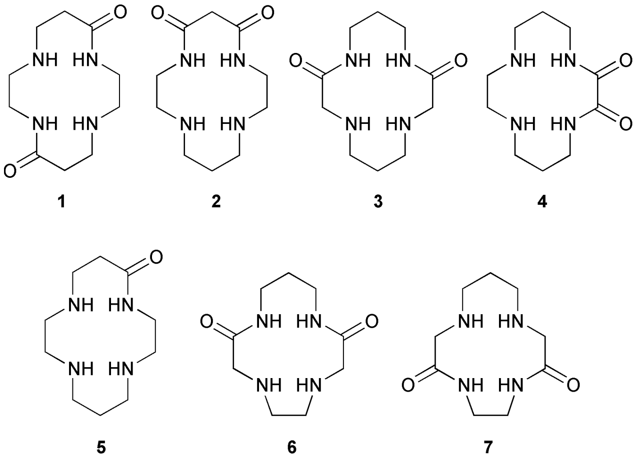

Scheme 1

Applications of *cis*-dioxocyclam and its derivatives are multiple. From a synthetic point of view, it is, thus far, the most convenient route towards C-substituted cyclam derivatives and 1,11-di-N-functionalized cyclam-based macrocycles can easily be obtained after reduction of the amide groups. They might be used, for instance, for selective extraction of platinum from aqueous metal ion mixtures[12] or as siderophore analogs.[13] Cobalt(II) and nickel(II) complexes of some dioxocyclams have shown interesting dioxygen uptake properties.[11,14] Nickel(II) complexes also catalyze the oxidation of alkenes.[15] The 1,4,8,11-tetraazacyclotetradecane-2,9-dione (**3**) isomer has been obtained using the crab-like cyclization reaction and its copper(II) complex has been studied.[16,17] Another isomer with two vicinal carbonyl groups, 1,4,8,11-tetraazacyclotetradecane-2,3-dione (**4**),[18] and its tetramethylated analog,[19] have been recently described.

In **2**, **3** and **4**, both amide functions are contiguous. A few dioxocyclam derivatives with *trans* amide groups have already been described in the literature, like the tricyclic lactam obtained by rearrangement of 1,8-bis(carboxymethyl)-1,4,8,11-tetraazacyclotetradecane. This compound, which can be considered as a reinforced 2,9-dioxocyclam, has been crystallographically characterized.[20,21] A functionalized 5,12-dioxocyclam has been obtained by dimerization, followed by reduction of a suitable azapenam.[22]

1,4,8,11-Tetraazacyclotetradecane-5,12-dione (**1**), also called 5,12-dioxocyclam or *trans*-dioxocyclam, has been isolated from the reaction of ethylenediamine and methylacrylate[23]

---

† For part III, see ref. 1.

DOI: 10.1039/b005052k

while the condensation of ethylenediamine and methyl methacrylate yielded the corresponding dimethylated derivative.[24] In contrast to the *cis* isomers, 5,12-dioxocyclam has yet only been used for synthetic purposes, as a synthon for the preparation of 1,8-disubstituted cyclams.[25,26] This compound constitutes an interesting starting material for the synthesis of new cryptands[27–29] and macrotricycles,[30,31] because it can be viewed as a *trans* "autodiprotected" cyclam. More recently, we were also able to obtain *trans* N-arylated derivatives of **1**.[32]

As part of our general interest in the coordination chemistry of tetraazamacrocycles, we are currently investigating the metal-binding ability of this ligand. As a biomimetic model of oligopeptides, its complexes should present interesting chemical and biological properties that may find applications in fields such as enzyme mimicry, stabilization of unusual oxidation states, ion separation or catalysis. Herein, we report the synthesis and characterization in solution of the free-base **1** together with a detailed conformational analysis of **1** in the crystalline state and of two corresponding diprotonated forms with two different counter anions, bromide and perchlorate. The protonation properties of **1** are discussed in light of those reported for various 13- and 14-membered analogs.

Results and discussion

Synthesis and spectroscopic characterization

The free-base 1,4,8,11-tetraazacyclotetradecane-5,12-dione was synthesized according to the procedure described by Tomalia and Wilson,[23] which relies on a [2 + 2] Michael condensation of methyl acrylate in neat ethylenediamine at temperatures close to 0 °C. The linear [1 + 1] addition product readily undergoes subsequent intermolecular and intramolecular amidation reactions to form first the linear dimer and then the cyclic diamide. Due to its lower solubility when compared to the open chain adducts, the cyclization reaction is carried out in aqueous solution. After 3 days, the reaction mixture is diluted with water and allowed to stand for an additional week at room temperature until the crude dioxocyclam precipitate is removed by filtration. Analytically pure compound was obtained in 2% yield after recrystallization in water.

The ^{1}H NMR spectrum in $CDCl_3$ shows a single set of six resonances. Four of them appear in the aliphatic CH_2 region, suggesting a C_i symmetric structure on the NMR time scale. Relying on the splitting pattern, the low-field doublet of triplets centered at 3.38 ppm is readily assigned to the methylene groups adjacent to the amide nitrogen atoms, whereas the most high-field-shifted triplet (2.39 ppm) is attributed to the protons located in the positions α to the carbonyl groups. A homodecoupling experiment enabled the assignment of the two remaining triplets appearing at 2.80 and 2.92 ppm to the methylene groups of the ethylenediamine and β-alaninamide moieties, respectively. As expected, the amide protons give rise to a broad singlet at 9.10 ppm. The integral and the chemical shift suggest that the second broad signal at 1.48 ppm arises from the four protons of the two cocrystallized water molecules, also evidenced by elemental analysis. Thus, both protons belonging to the secondary amines most probably give rise to a low-intensity signal that may overlap with the water peak.

The infrared spectrum of the free base exhibits the typical N–H and C=O stretching, and C–N–H bending modes of secondary amides at 3304, 1635 and 1556 cm^{-1}, respectively. Protonation of the amine nitrogen atoms gives rise to new absorption bands between 2700 and 2850 cm^{-1}, which are characteristic of the $HR_2N\text{–}H^+$ oscillator, while the amide C–N–H bending vibration is split into a doublet at 1570 and 1531 cm^{-1}. For $[H_2(\mathbf{1})]Br_2$, the carbonyl stretch shifts to higher energy by 21 cm^{-1}. The same trend, together with a splitting of the transition into a doublet (1656 and 1640 cm^{-1}), is observed when perchloric acid is used instead of hydrobromic acid. The Cl–O stretching band appears as a broad triplet between 1145 and 1089 cm^{-1}, which is an indication of hydrogen-bonded perchlorate anions.[33]

Protonation constants

The protonation constants, defined by eqn. (1), of the diprotic base 5,12-dioxocyclam were determined by means of potentiometric titrations carried out in aqueous 0.1 M KNO_3 solutions maintained at 25.0(1) °C.

$$LH_{n-1}^{(n-1)+} + H^+ \rightleftarrows LH_n^{n+}$$

$$K_{01n} = \frac{[LH_n^{n+}]}{[LH_{n-1}^{(n-1)+}][H^+]} \qquad (1)$$

$$\beta_{012} = K_{011}K_{012}$$

The mean values from three replicate determinations are log K_{011} = 7.60(1) and log K_{012} = 7.44(3) (Table 1), which give an average protonation constant (log K_{av}) of 7.52(3). Thus, each secondary amine of 5,12-dioxocyclam is about two orders of magnitude more acidic than the primary amine of β-alaninamide [log K_{011} = 9.20(1), $I = 0.1$, $T = 25$ °C].[34] Compared to cyclam, the presence of two electron-attracting endocyclic amide groups decreases the basicity of the two remaining amines by more than six orders of magnitude (log β_{012} = 15.04 and 21.7[34] for **1** and cyclam, respectively).

The first protonation constant found for **1** is in good agreement with the second protonation constant of the monoamide compound **5**, 1,4,8,11-tetraazacyclotetradecane-5-one [log K_{012} = 7.32(2)].[35] The value of log K_{011} also compares well with the corresponding value reported for isomer **3** [log K_{011} = 7.81(1)] and for two related 13-membered analogs of **3**, namely 1,4,7,10-tetraazacyclotridecane-2,9-dione (**6**) [log K_{011} = 7.21(2)] and 1,4,7,10-tetraazacyclotridecane-3,8-dione (**7**) [log K_{011} = 7.69(1)].[17] Among the three dioxocyclam isomers for which thermodynamic parameters have been determined, **2** is the most basic since the first protonation occurs at much higher pH [log K_{011} = 9.54(9)].[34] The enhancement of the basic character of **2** is a direct consequence of the larger distance between the protonation sites and the positively polarized carbon atoms belonging to the carbonyl groups.

The relative magnitude of the second protonation constant (K_{012}) reflects the free-energy cost of protonating an amine located close to a quaternary ammonium center. Several contributing factors might be listed, such as (*i*) the electrostatic repulsion between two positive charges, (*ii*) the breakup of a favorably chelated single proton shared between two amino nitrogen atoms and/or of hydrogen bonds, (*iii*) a conformational rearrangement of the ring structure, (*iv*) the solvation energy. Accordingly, **6** exhibits the most acidic amine [log K_{012} = 3.02(2)] and thus the largest separation between log

Table 1 Protonation constants of cyclam and various mono and dioxo derivatives

Ligand	log K_{011}	log K_{012}	log K_{011} − log K_{012}
1[a]	7.60(1)	7.44(3)	0.16
2[b]	9.54(9)	5.80(5)	3.74
3[c]	7.81(1)	5.68(2)	2.13
5[d]	10.87(2)	7.32(2)	3.55
		3.37(3)[e]	3.95[f]
Cyclam[b]	11.4(1)	10.3(1)	1.1
6[c]	7.21(2)	3.02(2)	4.19
7[c]	7.69(1)	5.90(1)	1.79

[a] $I = 0.1$ (KNO_3), $T = 25$ °C. [b] $I = 0.1$, $T = 25$ °C.[34] [c] $I = 0.1$ (KCl), $T = 25$ °C.[17] [d] $I = 0.5$ (KNO_3), $T = 25$ °C.[35] [e] log K_{013}. [f] log K_{012} − log K_{013}.

K_{011} and log K_{012} (4.19 log units) since both protonation sites belong to the same ethylenediamine moiety. The first proton is most probably shared between both contiguous ethylenediamine nitrogen atoms in $[H(\mathbf{6})]^+$, which severely hinders the second protonation. For the remaining compounds, the log K_{012} values increase in the following order: **3** [5.68(2)], **2** [5.80(5)], **7** [5.90(1)] and **1** [7.44(3)]. The wider distance between the pair of quaternary ammonium sites in the propylenediamine fragments of $[H_2(\mathbf{2})]^{2+}$, $[H_2(\mathbf{3})]^{2+}$ and $[H_2(\mathbf{7})]^{2+}$ weakens the coulombic repulsion interaction. Owing to the fact that both protonations occur in the same pH range for **1**, it may be inferred that the electrostatic repulsion between both *trans*-located amino groups is negligible. This observation also suggests that the macrocyclic framework undergoes only very limited structural changes upon each protonation step in solution, giving rise to a small entropy variation.

For two noninteracting sites having identical microscopic protonation constants, the difference between the successive macroscopic constants for both steps (log K_{011} − log K_{012}) would be equal to log 4 (=0.60) based on statistical considerations.[36] In the case of macrocycle **1**, this difference is significantly lower than the statistical factor. A limited number of systems giving rise to protonation cooperativity, in which protonation of the first site enhances the basicity of the second one, have been reported over the past decade.[34,37,38]

The acido-basic properties of the bridgehead tertiary amines belonging to a small bicyclic tris-urea cryptand provide such an example.[39] A conformational reorganization of the carbonyl groups, which rotate into the cavity and form hydrogen bonds with the first incoming proton, was invoked to explain the unusually high basicity of the second amine located on the opposite site. Assuming that the macrocycle **1** retains approximately its solid-state structure (*vide infra*) in solution as inferred from molecular dynamic simulations carried out on large-size protonated polyazacycloalkanes,[40] preorganization or hydrogen-bonding effects induced by structural rearrangements upon protonation might not account for the relative magnitude of the successive protonation constants.

The observed cooperativity in the protonation of **1** is reminiscent of the acido-basic behavior of some large polyazacycloalkanes belonging to the [3*k*]aneN$_k$ or [4*k*]aneN$_k$ series.[41] Indeed, the values of the first and second protonation constants become closer as the ring size and thus the flexibility increase. Obviously, neither electrostatic nor conformational arguments can explain this trend, which is characteristic of these families of compounds. Rather, the smaller than expected log K_{011} − log K_{012} difference might be rationalized in terms of solvation and interactions with the surrounding nitrate anions present in large excess in the bulk solution.[40] Considering the relative lipophilicity of the neutral free base, the net charge increase upon protonation enhances the water solubility of **1** and could result in a favorable hydration free-energy change. Accordingly, the observed cooperativity would be expected to be of entropic origin.[42,43]

However, one should also bear in mind that the separation of both protonation constants of **1** is close to the resolution limit of two overlapping equilibria and might therefore also be due, at least in part, to a mathematical artifact. Indeed, the absolute values of log K_{011} and log K_{012} should be considered with some caution since they were found to be highly correlated ($r \simeq 0.8$). Thus, their sum [log $\beta_{012} = 15.04(2)$] is known with more accuracy than their individual values.[44]

X-Ray structures

X-Ray quality crystals of 5,12-dioxocyclam and of two diprotonated forms, $[H_2(\mathbf{1})]Br_2$ and $[H_2(\mathbf{1})](ClO_4)_2$, were obtained as colorless rectangular blocks by slow evaporation of each compound from an aqueous solution. The nonprotonated bisamide and the dihydrobromic derivative crystallize in the centrosymmetric space group $P\bar{1}$ (Table 2) with a half molecular unit belonging to the asymmetric unit. Two water molecules were also found in the molecular unit of compound **1**, confirming the results of the elemental analysis. The dihydroperchlorate form $[H_2(\mathbf{1})](ClO_4)_2$ crystallizes in the centrosymmetric space group $P2_1/a$, revealing the presence of two independent half-molecules in the asymmetric unit. ORTEP[45] views of the macrocycle found in $\mathbf{1}\cdot 2H_2O$ and $[H_2(\mathbf{1})](ClO_4)_2$ are shown in Fig. 1, while relevant bond distances and bond angles are summarized in Table 3.

In order to facilitate the conformational analysis of the macrocycles, the sign and magnitude of the torsion angles are graphically displayed *vs.* the bond number in Fig. 2. Comparison of the resulting polar maps enables one to locate the corner positions by recognizing their characteristic torsion angle sequences and further allows a facile identification of the macrocyclic conformation. Following the original definition by Dale,[46] a corner is defined as the central atom of an *anti-gauche-gauche-anti* ($ag^{\pm}g^{\pm}a$) bond sequence where both successive *gauche* angles (ideally ±60°) are of the same sign. Alternatively, a pseudocorner may arise when both *gauche* bonds of the same *anti-gauche-gauche-anti* arrangement have opposite signs. A positive value of a torsion angle is assigned to a *gauche* bond if the rear bond is rotated clockwise with respect to the front bond when looking along the central bond axis.[47] According to Dale's nomenclature, each conformation is designated by a series of numbers in square brackets, each digit corresponding to the number of chemical bonds found

Table 2 Crystal data for **1** and its two diprotonated forms $[H_2(\mathbf{1})]Br_2$ and $[H_2(\mathbf{1})](ClO_4)_2$

Formula	$C_{10}H_{20}N_4O_2\cdot 2H_2O$	$C_{10}H_{22}N_4O_2Br_2$	$C_{10}H_{22}N_4O_{10}Cl_2$
M_w	264.33	390.14	429.22
Crystal system	Triclinic	Triclinic	Monoclinic
Space group	$P\bar{1}$	$P\bar{1}$	$P2_1/a$
a/Å	7.559(2)	5.2851(2)	10.2700(2)
b/Å	4.997(2)	8.0718(4)	16.1690(4)
c/Å	10.293(2)	9.5424(5)	10.8995(2)
α/°	116.96(3)	109.126(3)	90
β/°	91.55(3)	104.189(4)	106.900(1)
γ/°	100.31(3)	97.989(3)	90
U/Å^3	338.4(2)	362.03(3)	1731.76(6)
Z	1	1	4
T/K	293(2)	112(2)	112(2)
μ(Mo-Kα)/mm^{-1}	0.100	5.600	0.436
No of collected reflns	1163	2142 [R(int) = 0.033]	7487 [R(int) = 0.022]
No of unique reflns	1163	1619	4881
R_1, R_2 [$I > 2\sigma(I)$][a]	0.0328, 0.0924	0.0255, 0.0670	0.0316, 0.0812

[a] $R_1 = \Sigma\,\|F_0| - |F_c\|/\Sigma|F_0|$, $R_2 = \{\Sigma[w(F_0^2 - F_c^2)^2]/\Sigma[wF_0^4]\}^{1/2}$.

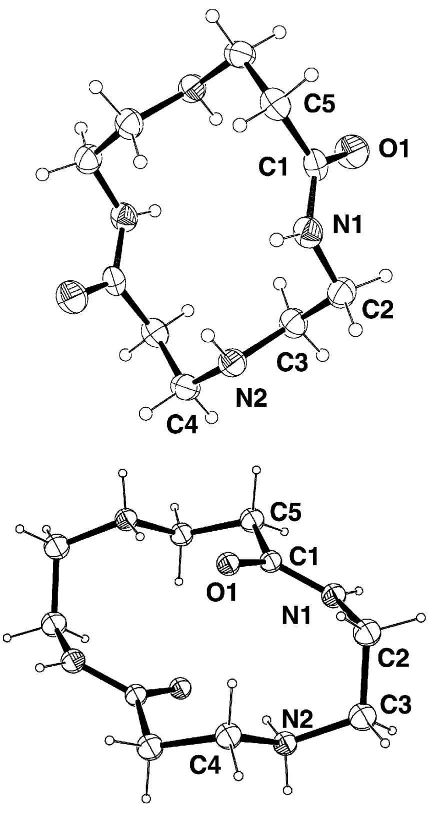

Fig. 1 ORTEP views of the macrocycle found in $1 \cdot 2H_2O$ (top) and $[H_2(\mathbf{1})](ClO_4)_2$ (bottom), showing thermal ellipsoids at 50% probability level and the numbering scheme for one-half of the molecule only (the symmetry related atoms are labeled according to the same scheme and primed).

between consecutive corner atoms.[48–50] Although well adapted to describe the conformation adopted by cyclic polyalkanes, this description becomes ambiguous for macrocycles containing heteroatoms.[51] A detailed stereochemical analysis of such structures requires that the position of the heteroatoms within the cycle be taken into account, in order to distinguish the different conformers possessing the same torsion angle sequences. In a recent review, each of these stereoisomers has been differentiated for the first time.[52] Maintaining the informative nomenclature introduced by Dale, the exact location of the nitrogen atoms with respect to the corners was designated by adding a capital letter.

Following this new classification, the bisamide rings in $1 \cdot 2H_2O$ and $[H_2(\mathbf{1})]Br_2$ display a quadrangular [3,4,3,4]-B conformation in which the nitrogen atoms are endocyclic. As evidenced by the polar map shown in Fig. 2, these are positioned one bond away from a corner position occupied by the C2, C4, C2′ or C4′ methylenic carbon atoms. Despite their striking similarity, superposition of the protonated and nonprotonated molecules shows some conformational differences (Fig. 3). A least-squares fitting of the 16 non-hydrogen atoms belonging to the macrocycles gives a root mean square deviation (rmsd) of 0.413 Å. As seen in Fig. 3, the major deviations occur in the tilting of the carbonyl groups, giving rise to a set of C5–C1–N1–C2 torsion angles of similar magnitude but opposite sign (τ_6 and τ_{13} in Fig. 2). The internal angle between the mean plane defined by the C5–C1–O1–N1 atoms {rmsd of 0.0002 and 0.0005 Å for $1 \cdot 2H_2O$ and $[H_2(\mathbf{1})]Br_2$, respectively} and the plane passing through the four corner positions C2–C4–C2′–C4′ is wider open for $1 \cdot 2H_2O$ [105.4(1)°] than for $[H_2(\mathbf{1})]Br_2$ [89.1(1)°], where the carbonyl bonds point in a perpendicular direction with respect to the macrocyclic skeleton.

As revealed by the crystallographic study of $[H_2(\mathbf{1})](ClO_4)_2$, protonated 5,12-dioxocyclam is able to adopt a variety of stable conformations, depending on the counter anion. The two independent macrocycles found in the structure exhibit essentially identical conformations, their overlay producing a rmsd of 0.071 Å (Fig. 3). The main difference appears again in the carbonyl group orientation. The cycles show a quadrangular [3,4,3,4]-C arrangement where the exocyclic amide nitrogen atom N1 is located two bonds away from the adjacent corner atoms C3 and C5, while the amine nitrogen atom N2 is located one bond away from the cor-

Table 3 Selected bond lengths (Å) and angles (°) for **1** and its two diprotonated forms $[H_2(\mathbf{1})]Br_2$ and $[H_2(\mathbf{1})](ClO_4)_2$[a]

	$1 \cdot 2H_2O$	$[H_2(\mathbf{1})]Br_2$	$[H_2(\mathbf{1})](ClO_4)_2$[a]	
O1–C1	1.264(2)	1.233(3)	1.242(2)	1.243(2)
N1–C1	1.342(2)	1.342(3)	1.341(2)	1.338(2)
N1–C2	1.453(2)	1.458(3)	1.454(2)	1.459(2)
N2–C3	1.500(2)	1.490(3)	1.494(2)	1.497(2)
N2–C4	1.462(2)	1.501(3)	1.498(2)	1.499(2)
C1–C5	1.513(2)	1.511(3)	1.514(2)	1.517(2)
C2–C3	1.509(2)	1.521(3)	1.516(2)	1.525(2)
C4–C5′	1.527(2)[(i)]	1.522(3)[(ii)]	1.520(2)[(iii)]	1.528(2)[(iv)]
C1–N1–C2	121.4(2)	120.5(2)	121.8(1)	122.7(1)
C3–N2–C4	113.6(1)	115.5(2)	116.2(1)	115.2(1)
O1–C1–N1	122.9(1)	122.3(2)	122.1(1)	122.5(1)
O1–C1–C5	122.0(1)	120.7(2)	120.5(1)	120.3(1)
N1–C1–C5	115.1(1)	117.0(2)	117.4(1)	117.3(1)
N1–C2–C3	112.1(1)	113.0(2)	113.3(1)	113.23(9)
N2–C3–C2	111.3(1)	111.3(2)	113.2(1)	112.35(9)
N2–C4–C5′	116.4(1)[(i)]	113.0(2)[(ii)]	110.6(1)[(iii)]	111.6(1)[(iv)]
C1–C5–C4′	110.8(1)[(i)]	112.3(2)[(ii)]	113.2(1)[(iii)]	112.5(1)[(iv)]

[a] Symmetry transformations used to generate equivalent atoms: (*i*) $2 - x, 1 - y, -z$; (*ii*) $-x, -y + 1, -z$; (*iii*) $-x + 1, -y, -z + 2$; (*iv*) $-x + 1, -y, -z + 1$. [b] $[H_2(\mathbf{1})](ClO_4)_2$ crystallizes with two nonsymmetry-related half-molecules in the asymmetric unit.

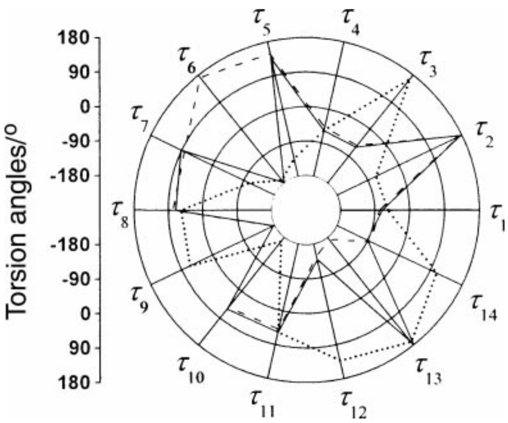

Fig. 2 Polar maps displaying the torsion angle sequence of molecules $1 \cdot 2H_2O$ (——), $[H_2(\mathbf{1})]Br_2$ (– –) and $[H_2(\mathbf{1})](ClO_4)_2$ (· · ·). τ_1 is defined as the N1–C2–C3–N2 torsion angle, the following angles being obtained by a clockwise circular permutation around the macrocyclic ring of 5,12-dioxocyclam.

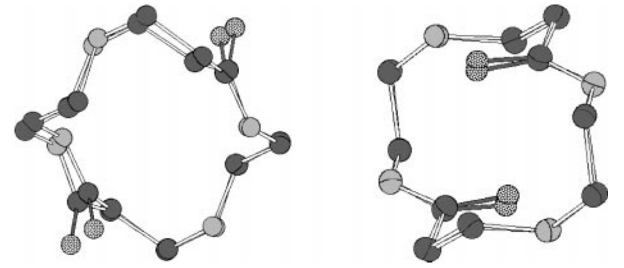

Fig. 3 CHEM3D overlay of the bisamide rings in $1 \cdot 2H_2O$ and $[H_2(\mathbf{1})]Br_2$ (left) and of both nonsymmetry related molecules of $[H_2(\mathbf{1})](ClO_4)_2$ (right). The rms deviation in 16 atom positions is 0.413 and 0.071 Å, respectively (hydrogen atoms are omitted).

responding corner atom C3 and two bonds away from C5′. The present study highlights the strong effect on the overall ring conformation of the relative orientation of both carbonyl moieties with respect to the macrocyclic cavity. As found for **1**$\cdot$2H$_2$O and [H$_2$(**1**)]Br$_2$, the amide groups take the most stable *Z* arrangement. However, in the case of [H$_2$(**1**)](ClO$_4$)$_2$ the carbonyl bonds point towards the cavity, the mean amide plane (rmsd of 0.0023 Å) being rotated by 39.5(5)° and 44.7(5)° away from the C3–C5–C3′–C5′ plane for the two independent molecules present in the asymmetric unit. The origin of this displacement may be found in the different environments observed for the nonsymmetry related macrocycles in the unit cell, which give rise to distinct hydrogen bond interactions around the carbonyl oxygen atoms O1A and O1B (*vide infra*). Likewise, three of the four possible [3,4,3,4] conformers have been structurally characterized in the case of tetraprotonated cyclam salt.[52]

The directionality of each N–R bond (*i.e.* R = H in the present case) is unique when the nitrogen atom is not occupying a vertex position, while a substituent attached to a nitrogen atom located at a corner or a pseudo-corner can point in two possible directions (above or below the mean plane encompassing the four nitrogen atoms). Thus, the configuration of the four nitrogen atoms is imposed by the three-dimensional macrocyclic layout when the adopted conformation is either [3,4,3,4]-B or [3,4,3,4]-C. Obviously, there is a direct, and yet unrecognized, relationship between Dale's description of macrocyclic conformations and the stereochemical classification of 1,4,8,11-tetraazacyclotetradecane introduced by Bosnich *et al.*[53] in the mid sixties. Most intriguingly, this widely employed denomination relies solely on the relative orientation (*i.e.* chirality) of the four N–R bonds with respect to the N$_4$ mean plane without considering the topography of the macrocyclic chain. It can be easily recognized from Fig. 4 that 14-membered cycloalkanes displaying a [3,4,3,4]-B or [3,4,3,4]-C conformation can only adopt a type IV geometry according to Bosnich's formalism (*i.e.* both pairs of adjacent N–H bonds belonging to ethylenediamine moieties point in opposite directions).

For the three structures, the average C(sp^3)–C(sp^3) [1.518(7) Å], C(sp^3)–N [1.456(3) Å] and carbonyl C(sp^2)–N [1.341(3) Å] distances are typical of acyclic secondary amides.[54] The high quality diffraction data enabled us to localize at reasonable bonding distances all the hydrogen atoms in the Fourier difference maps at the end of the refinement process and consequently to ascertain the protonation of the N2 atoms in [H$_2$(**1**)]Br$_2$ and [H$_2$(**1**)](ClO$_4$)$_2$. The presence of quaternary ammonium sites in these compounds is further corroborated by the fact that the N2–C3 and N2–C4 distances are statistically equal and average to 1.497(4) Å. In contrast, the two carbon–amino nitrogen bond lengths differ significantly in the structure of **1**, with C3–N2 = 1.500(2) Å and C4–N2 = 1.462(2) Å. While this difference in bond lengths is somewhat surprising, the value of the C4–N2 distance is typical of nonprotonated amines in cyclam derivatives.[52] The same discrepancy is also observed for both angles involving the secondary amine nitrogen atom, namely the N2–C3–C2 [111.3(3)°] and N2–C4–C5′ [116.4(1)°] angles. A possible explanation could rely on the formation of two intermolecular hydrogen bonds (Table 4): one between N2 and one cocrystallized water molecule [O3$\cdots$N2 = 2.865(2) Å, O3–H6$\cdots$N2 = 164(3)°] and the second between N1–H1 and the carbonyl oxygen atom O1 [N1$\cdots$O1 = 2.933(2) Å, N1–H1$\cdots$O1 = 165(2)°] belonging to an adjacent molecule generated by the symmetry transformation (*x*, 1 + *y*, *z*). These hydrogen bonds could displace the amino nitrogen atom N2 from its usual equidistant position between carbon atoms C3 and C4, giving rise to a lengthening of the C3–N2 bond and a concomitant opening of the N2–C4–C5′ angle.

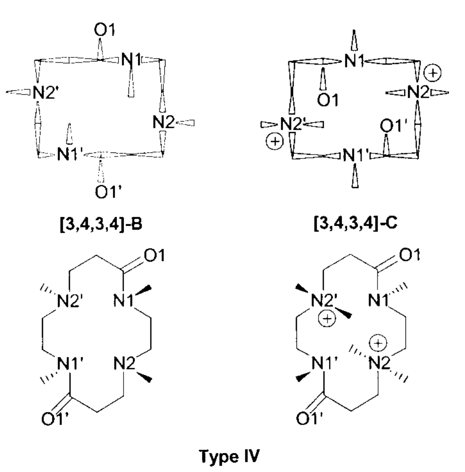

Fig. 4 Idealized wedge-type drawings of the quadrangular [3,4,3,4]-B and [3,4,3,4]-C conformations showing the unique relationship with Bosnich's stereochemical representation of a type IV cyclam derivative.

In all cases, the crystalline cohesion is mainly driven by a network of hydrogen bonds. The crystal packing of both the nonprotonated bisamide **1** and the dihydrobromic derivative [H$_2$(**1**)]Br$_2$ is almost equivalent. Macrocycles stack along the shorter unit-cell axis (*b* = 4.997 and *a* = 5.2851 Å, respectively) by means of C=O$\cdots$H–N hydrogen bonds forming molecular channels. The water molecules or bromine anions are located between the parallel running chains of macrocycles (Fig. 5), giving rise to a tridimensional network of hydrogen bonds between neighboring stacks and the intercalated water molecules or anions.

Compared to **1** and [H$_2$(**1**)]Br$_2$, the crystal packing of [H$_2$(**1**)](ClO$_4$)$_2$ (Fig. 6) shows basically the same features. The main difference is related to the unit-cell axis along which the stacking of macrocycles takes place: the presence of two independent molecules in the crystal structure of [H$_2$(**1**)](ClO$_4$)$_2$ induces a doubling of the cell parameter in the *c* axis direction (*c* = 10.8995 Å).

The relevant hydrogen bonding contacts found in the crystal structures are reported in Table 4. Among them, the strongest interaction systematically involves the carbonyl oxygen atom O1 as acceptor. In [H$_2$(**1**)]Br$_2$ and

Table 4 Intermolecular hydrogen bond distances (Å) and angles (°) for **1** and its two diprotonated forms [H$_2$(**1**)]Br$_2$ and [H$_2$(**1**)](ClO$_4$)$_2$[a]

D–H$\cdots$A	*d*(D–H)	*d*(H$\cdots$A)	*d*(D$\cdots$A)	∠(DHA)
1$\cdot$2H$_2$O				
N1–H1$\cdots$O1$^{(i)}$	0.85(3)	2.10(3)	2.933(2)	165(2)
N2–H2$\cdots$O1$^{(i)}$	0.91(2)	2.59(2)	3.435(2)	156(1)
O3–H6$\cdots$N2	0.65(2)	2.23(2)	2.865(2)	164(3)
[H$_2$(**1**)]Br$_2$				
N1–HN1$\cdots$Br1$^{(ii)}$	0.87(3)	2.67(3)	3.466(2)	153(3)
N2–HN2$\cdots$O1$^{(ii)}$	0.85(3)	2.04(3)	2.825(3)	153(3)
N2–HN2$\cdots$O1$^{(iii)}$	0.85(3)	2.46(3)	2.990(3)	121(3)
N2–HN3$\cdots$Br1$^{(iv)}$	0.89(3)	2.39(3)	3.251(2)	162(3)
[H$_2$(**1**)](ClO$_4$)$_2$				
N1A–HN1A$\cdots$O2$^{(v)}$	0.87(2)	2.18(2)	3.052(2)	174(2)
N1B–HN1B$\cdots$O6$^{(vi)}$	0.80(2)	2.35(2)	3.083(2)	153(2)
N2B–HN2B$\cdots$O9$^{(vi)}$	0.89(2)	2.36(2)	2.991(2)	128(1)
N2A–HN2A$\cdots$O1A$^{(vii)}$	0.90(2)	1.94(2)	2.715(2)	142(2)
N2A–NH3A$\cdots$O9$^{(viii)}$	0.89(2)	1.98(2)	2.856(2)	169(2)
N2B–HN2B$\cdots$O1B$^{(ix)}$	0.89(2)	2.03(2)	2.752(1)	137(2)
N2B–HN3B$\cdots$O4$^{(ix)}$	0.90(2)	2.14(2)	2.934(1)	147(2)
N2B–HN3B$\cdots$O5$^{(ix)}$	0.90(2)	2.41(2)	3.216(2)	149(1)

[a] Symmetry transformations used to generate equivalent atoms: (*i*) $x, y+1, z$; (*ii*) $x-1, y, z$; (*iii*) $-x, -y+1, -z$; (*iv*) $-x, -y, -z$; (*v*) $x+1/2, -y+1/2, z+1$; (*vi*) $x+1/2, -y+1/2, z$; (*vii*) $-x+1, -y, -z+2$; (*viii*) $-x+1/2, y-1/2, -z+2$; (*ix*) $-x+1, -y, -z+1$.

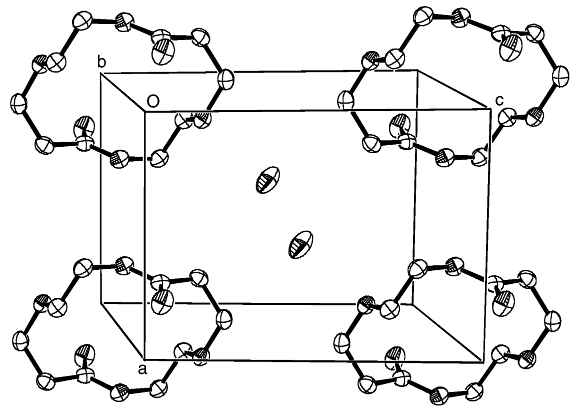

Fig. 5 Projection down the crystallographic *b* axis of the $[H_2(\mathbf{1})]Br_2$ structure showing the crystal packing and the outline of one unit cell.

$[H_2(\mathbf{1})](ClO_4)_2$, O1 is hydrogen bonded to the protonated N2 nitrogen atom. The C1–O1 distances are significantly shorter in the protonated structures (ranging from 1.233 to 1.243 Å) when compared to the nonprotonated molecule (1.264 Å). This indicates both a higher electron density in the C1–O1 bonds and a more important charge associated with the O1 atoms for the former compounds. Thus, the stronger interaction between the carbonyl oxygen and the surrounding atoms in the protonated structures is reflected by shorter H···O hydrogen bonding distances compared to the nonprotonated compound and should lead to significant shifts towards higher frequencies of the carbonyl stretching vibration.

As expected, the shortest C=O distance {1.233 Å for $[H_2(\mathbf{1})]Br_2$} correlates well with the infrared data recorded for that compound, since the corresponding ν_{CO} band shifts to higher energy by 21 cm^{-1}. In the case of $[H_2(\mathbf{1})](ClO_4)_2$, both crystallographically independent molecules present in the cell exhibit slightly longer and statistically equivalent C=O bond lengths [1.242(2) and 1.243(2) Å]. The shift to higher wavenumbers of the C=O band upon protonation of the ligand with perchloric acid is therefore expected to be less important. Moreover, splitting of the band into a doublet (1656 and 1640 cm^{-1}) is experimentally observed, which might be related to the different environments surrounding the O1 atoms in both independent molecules, namely their respective hydrogen bonding patterns (Table 4).

In order to discuss this point further, the position of the hydrogen atoms involved in the hydrogen bonds must be accurately known. Although all the protons could be localized in the difference Fourier maps, their exact position with respect to the heavy atom cannot be determined by X-ray diffraction experiments. As a first approximation, the N^+–H distances were recalculated by placing the hydrogen atoms at the mean bonded distance observed from neutron diffraction experiments (N^+–H = 1.033 Å).[54] In this way, the N2A–HN2A···O1A and N2B–HN2B···O1B hydrogen bonding distances change from 1.94 and 2.03 Å to the more precise values 1.84 and 1.93 Å, respectively. Based on a previous study that established the relationship between the dissociation energy D_E (in kJ mol^{-1}) and the H···O interaction distance $r_{H\cdots O}$ (in Å) of X–H···O hydrogen bonds (X = C, N or O), $D_E = 25\,000 \exp(-3.6\ r_{H\cdots O})$,[55] the energy difference between both hydrogen bond interactions is close to 9.2 kJ mol^{-1}. This significant difference correlates with the presence of two carbonyl stretching bands in the infrared spectrum of $[H_2(\mathbf{2})](ClO_4)_2$ separated by 16 cm^{-1}.

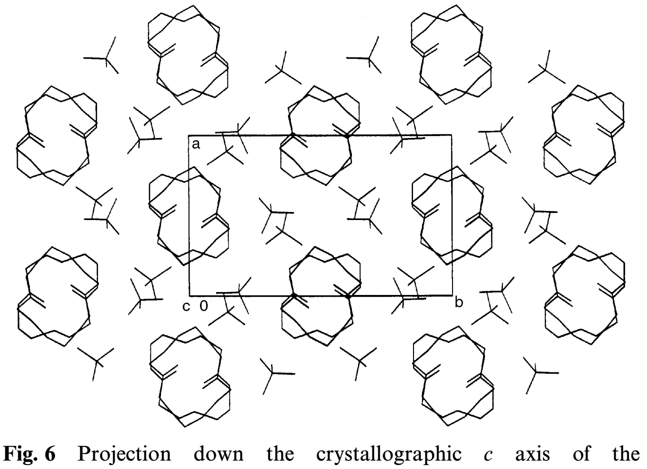

Fig. 6 Projection down the crystallographic *c* axis of the $[H_2(\mathbf{1})](ClO_4)_2$ structure showing the crystal packing and the outline of one unit cell.

In conclusion, the spectroscopic and crystallographic investigations undertaken in the present work have shown that the structural features of 5,12-dioxocyclam and its protonated forms are mainly controlled by the crystal packing forces. As evidenced by the potentiometric data, protonation of the secondary amines induces only limited conformational changes in agreement with their optimized separation (N2···N2′ = 5.32–5.57 Å) in any of the quadrangular [3,4,3,4] conformations. The major factor to be considered to explain the subtle structural variations observed for the three compounds is the intermolecular hydrogen bond network that involves the oxo groups, the amine sites of adjacent molecules, and the surrounding anions in the crystal lattice. Finally, the reported results also afford new guidelines for understanding the peculiar reactivity of this "autodiprotected" cyclam derivative towards electrophilic reactants, allowing the synthesis of numerous cross-bridged macrocycles and barrel-shaped macrotricycles.

Experimental

General

Unless otherwise noted, all reagents of analytical grade were obtained from commercial suppliers and used without further purification. ^1H and $^{13}C\{^1H\}$ NMR spectra were recorded on a Bruker AC 200 superconducting Fourier transform spectrometer operating at 200.13 and 50.03 MHz, respectively, at the Centre de Spectroscopie Moléculaire de l'Université de Bourgogne. All chemical shifts were referenced to the solvent peak. Infrared spectra were measured as KBr pellets from 4000 to 400 cm^{-1} on a Bruker IFS 66v Fourier transform spectrometer. MALDI-TOF mass spectra were obtained on a Bruker ProFLEX III spectrometer using dithranol as the matrix. Microanalyses were performed on a Fisons EA 1108 CHNS instrument or by the Service Central d'Analyse du Centre National de la Recherche Scientifique, Vernaison, France.

Synthesis

1,4,8,11-Tetraazacyclotetradecane-5,12-dione (1). To 5.6 L (83.57 mol) ethylenediamine maintained at 0 °C, 7.5 L (83.57 mol) methyl acrylate are added drop-wise over a period of 8 h. The reaction mixture is then allowed to reach room temperature and is stirred for 3 additional days. The cyclization reaction is carried out in aqueous solution by dropping in 3.5 L of distilled water. After 6 more days of stirring, the white precipitate is recovered by filtration, recrystallized in water and dried (172 g, 1.8%). Anal. Found: C, 44.94; H, 9.15; N, 21.75; O, 24.22. $C_{10}H_{20}N_4O_2 \cdot 2H_2O$ requires C, 45.44; H, 9.15; N, 21.20; O, 24.21%. $\tilde{\nu}_{max}/cm^{-1}$: 3304 (br, ν_{NH}), 2975 (ν_{CH_2}), 2948 (ν_{CH_2}), 2925 (ν_{CH_2}), 2868 (ν_{CH_2}), 1635 (ν_{CO}) and 1556 (δ_{CNH}); δ_H(200 MHz, $CDCl_3$): 1.48 (br s; 4H; H_2O), 2.39 (t, ^3J = 5.6 Hz; 4H; $COCH_2$), 2.80 (t, ^3J = 5.2 Hz; 4H; $CONHCH_2CH_2$), 2.92 (t, ^3J = 5.6 Hz; 4H; $COCH_2CH_2$) and

3.38 (dt, $^3J = 5.2$ Hz; 4H; CONHCH_2); δ_C(50 MHz, $CDCl_3$): 35.5, 38.6, 45.8, 48.5 and 172.7; MALDI-TOF MS *m/z*: 229 $[M + H]^+$, 251 $[M + Na]^+$.

1,4,8,11-Tetraazacyclotetradecane-5,12-dione dihydrobromide, $[H_2(1)]Br_2$. Dioxocyclam (200 mg, 0.757 mmol) is dissolved in 50 mL hot methanol. After dissolution, addition of 1 mL of a concentrated HBr solution leads to the formation of a white precipitate that is filtered off, washed with cold methanol and dried under vacuum (280 mg, 95%). X-Ray quality crystals were obtained by slow evaporation of a saturated aqueous solution. Anal. Found: C, 31.24; H, 5.88; N, 14.03. $C_{10}H_{20}N_4O_2 \cdot 2HBr$ requires C, 30.79; H, 5.68; N, 14.36%. $\tilde{\nu}_{max}/cm^{-1}$: 3257 (br, ν_{NH}), 3139 (br, ν_{NH}), 2939 (ν_{CH_2}), 2849 (ν_{CH_2}), 2757 (br, ν_{NH^+}), 1656 (ν_{CO}), 1570 (δ_{CNH}) and 1531 (δ_{CNH}).

1,4,8,11-Tetraazacyclotetradecane-5,12-dione dihydroperchlorate, $[H_2(1)](ClO_4)_2$. After dissolution of 200 mg (0.757 mmol) of dioxocyclam in 50 mL water, 1 mL of a concentrated $HClO_4$ solution is added. Colorless, prismatic crystals of diprotonated dioxocyclam suitable for X-ray diffraction studies were obtained by slow evaporation of the reaction mixture. Anal. Found: C, 28.63; H, 5.52; N, 12.88. $C_{10}H_{20}N_4O_2 \cdot 2HClO_4$ requires C, 27.98; H, 5.17; N, 13.05%. $\tilde{\nu}_{max}/cm^{-1}$: 3192 (br, ν_{NH}), 3067 (br, ν_{NH}), 2941 (ν_{CH_2}), 2849 (ν_{CH_2}), 2778 (br, ν_{NH^+}), 1656 (ν_{CO}), 1640 (ν_{CO}), 1570 (δ_{CNH}), 1533 (δ_{CNH}), 1145 ($\nu_{ClO_4^-}$), 1115 ($\nu_{ClO_4^-}$) and 1089 ($\nu_{ClO_4^-}$).

Potentiometric titrations

All solutions were prepared with deionized water further purified by passage through an Elgastat UHQII (Elga) ion-exchange cartridge system (resistivity 18 MΩ cm) and then boiled for 2 h while being purged with argon. Titrant solutions were stored under an atmosphere of purified argon using Ascarite II (Acros, 20–30 mesh) scrubbers in order to prevent absorption of carbon dioxide. Carbonate-free 0.1 M KOH was prepared from Merck concentrate (Titrisol®) and was standardized by titrating against oven-dried (120 °C for 2 h) potassium hydrogen phthalate (Aldrich, 99.99%) using a combined Ag/AgCl glass semi-microelectrode (Mettler-Toledo) filled with a solution saturated with KCl and AgCl. Equivalent points were calculated by the second-derivative method. Solutions of 0.1 M HNO_3 were similarly prepared and were standardized by titrating against oven-dried (120 °C for 2 h) TRIS buffer (Aldrich, 99.9%). All titrations were performed using a calibrated T110 (Schott) piston burette equipped with a TA10 interchangeable unit of 10 mL and a TR250 (Schott) data acquisition unit, both instruments being controlled by TR600 software (release 5.2) running on an IBM-compatible PC computer. Solutions were maintained under argon atmosphere at constant ionic strength ($I = 0.1$ KNO_3) and temperature [25.0(1) °C] by using a jacketed titration vessel fitted to a Lauda RE 106 water bath.

Protonation constants were determined by pH-metric measurements by using a XG100 (Radiometer–Tacussel) glass electrode and a XR110 (Radiometer–Tacussel) KCl-saturated calomel electrode. The reference electrode was separated from the bulk of the solution by a sintered-glass bridge filled with a 0.1 M KNO_3 solution. Before each titration, the electrode system was calibrated in hydrogen ion concentration units ($p[H] = -\log[H^+]$) by titrating 4.00 mL of standardized HNO_3 diluted in 25 mL of 0.100 M KNO_3 with standardized KOH. The titration data comprised between p[H] 1.86 to 2.65 and 10.97 to 11.89 were processed by nonlinear least-squares minimization procedures available in Microsoft Excel 5.0 in order to calculate the standard cell potential (E^0), the Nernst slope (S), together with the correction terms accounting for the changes in liquid junction potential in strongly acid (J_a) and alkaline (J_b) media. The sum of the unweighted square residuals on the observed emf readings (E_{mes}) is minimized according to the modified Nernst equation: $E_{mes} = E^0 + S\log[H^+] + J_a[H^+] + J_bK_w[H^+]^{-1}$. In addition, the base-concentration factor (γ) was also allowed to refine, whereas the ionic product of water was fixed ($pK_w = 13.78$ in 0.1 M KNO_3 at 25 °C).[34] Calibration data were rejected when the standard deviation of the residuals exceeded 0.12 mV. The emf readings recorded for the subsequent titration were converted with the help of an Microsoft Excel 5.0 spreadsheet into p[H] values by iterative solving of the equation: $p[H] = (E^0 - E_{mes} + J_a[H^+] + J_bK_w[H^+]^{-1})/S$. The protonation constants were refined by the weighted nonlinear least-squares program Hyperquad 2000 for Windows NT.[56] In the final refinement step, the total amounts of titrated ligand and initially added acid were also allowed to vary. All presented results are the average of at least three independent titrations. The standard deviations of the stepwise protonation constants (log *K*'s) were derived from the full variance/covariance matrix of the refined global constants (log β's).[44]

Crystal structure solution and refinement

High-quality, colorless single-crystal specimens of prismatic shape {0.30 × 0.22 × 0.14 mm for **1**, 0.14 × 0.10 × 0.10 mm for $[H_2(\mathbf{1})]Br_2$, and 0.25 × 0.12 × 0.12 mm for $[H_2(\mathbf{1})](ClO_4)_2$} were selected for the X-ray diffraction experiments. The X-ray source was graphite monochromatized Mo-Kα radiation ($\lambda = 0.710\,73$ Å) from a sealed tube. Measurements were collected at room temperature on a Stoe AED-2 (**1**) or at 112(2) K on a Nonius Kappa CCD diffractometer equipped with a nitrogen cryostream cooler from Oxford Cryosystems {$[H_2(\mathbf{1})]Br_2$ and $[H_2(\mathbf{1})](ClO_4)_2$}. Intensity data were recorded as $\omega - \theta$ scan profiles (**1**), or φ and ω scans with κ offsets {$[H_2(\mathbf{1})]Br_2$ and $[H_2(\mathbf{1})](ClO_4)_2$} up to a resolution of $(\sin\theta)/\lambda = 0.59$, 0.65 and 0.70 $Å^{-1}$, respectively. No significant intensity decay was observed during the data collections. No diffractometer or temperature problems occurred during the experiments. No significant absorption effects were observed in any case, in particular for the quite small and roughly isotropic $[H_2(\mathbf{1})]Br_2$ crystal, in spite of its high linear absorption coefficient [μ(Mo-Kα) = 5.6 mm^{-1}]. Data reduction was done using the commercial software X-RED release 1.19[57] (**1**) or DENZO[58] {$[H_2(\mathbf{1})]Br_2$ and $[H_2(\mathbf{1})](ClO_4)_2$}.

The three structures were solved by direct methods using the SHELXS97 program,[59] the best phase set gave all the positions for the non-H atoms in the diprotonated forms. Refinements were carried out by full-matrix least squares on F^2 using the SHELXL97 program,[60] and the complete set of reflections. Anisotropic thermal parameters were used for non-H atoms. In all cases, the hydrogen atoms were located by Fourier synthesis except for one belonging to a water molecule. In the case of the free-base form of **1**, all hydrogen atoms were refined with independent isotropic thermal factors. For both protonated structures, the N–H hydrogen atoms were refined with isotropic thermal factors constrained to 1.2 times the equivalent isotropic thermal factor of their respective bonded atom, while the C–H hydrogen atoms were refined with a riding model and a global isotropic temperature factor.

CCDC reference number 440/217. See http://www.rsc.org/suppdata/nj/b0/b005052k/ for crystallographic files in .cif format.

Acknowledgements

Dr Peter Gans (University of Leeds) is thanked for helpful advice and stimulating discussions on potentiometric data refinements. This work was supported by the Centre National de la Recherche Scientifique (CNRS) and the Conseil Régional de Bourgogne. L. F. thanks the Ministère de l'Education

National, de la Recherche et de la Technologie for a Ph.D. scholarship and E. E. gratefully acknowledges the CNRS for a research grant (poste rouge).

References

1 For the previous paper in this series, see C. Bucher, E. Duval, J. M. Barbe, J. N. Verpeaux, C. Amatore and R. Guilard, *C. R. Acad. Sci., Sér. IIc: Chim.*, 2000, **3**, 211.
2 E. Kimura, *J. Coord. Chem.*, 1986, **15**, 1.
3 I. Tabushi, Y. Taniguchi and H. Kato, *Tetrahedron Lett.*, 1977, **12**, 1049.
4 M. Kodama and E. Kimura, *J. Chem. Soc., Dalton Trans.*, 1979, 325.
5 M. Kodama, T. Yatsunami and E. Kimura, *J. Chem. Soc., Dalton Trans.*, 1979, 1783.
6 H. Sigel and R. B. Martin, *Chem. Rev.*, 1982, **82**, 385.
7 L. Fabbrizzi, F. Forlini, A. Perotti and B. Seghi, *Inorg. Chem.*, 1984, **23**, 807.
8 E. Kimura, T. Koike, H. Nada and Y. Iitaka, *Inorg. Chem.*, 1988, **27**, 1036.
9 X. H. Bu, Z. H. Zhang, X. C. Cao, S. Y. Ma and T. C. Chen, *Polyhedron*, 1997, **16**, 3525.
10 S. Zhu, F. Kou, H. Lin, C. Lin, M. Lin and Y. Chen, *Inorg. Chem.*, 1996, **35**, 5851.
11 E. Kimura, M. Sasada, M. Shionoya, T. Koike, H. Kurosaki and M. Shiro, *J. Biol. Inorg. Chem.*, 1997, **2**, 74.
12 E. Kimura, Y. Lin, R. Machida and H. Zenda, *J. Chem. Soc., Chem. Commun.*, 1986, 1020.
13 M. A. Santos, M. Gaspar, M. L. S. Gonçalves and M. T. Amorin, *Inorg. Chim. Acta*, 1998, **278**, 51.
14 R. Machida, E. Kimura and M. Kodama, *Inorg. Chem.*, 1983, **22**, 2055.
15 T. R. Wagler, Y. Fang and C. J. Burrows, *J. Org. Chem.*, 1989, **54**, 1548.
16 J. S. Bradshaw, K. E. Krakowiak, R. M. Izatt and D. J. Zamecka–Krakowiak, *Tetrahedron Lett.*, 1990, **31**, 1077.
17 R. J. Motekaitis, Y. Z. Sun, A. E. Martell and M. J. Welch, *Can. J. Chem.*, 1999, **77**, 614.
18 L. Cronin, A. R. Mount, S. Parsons and N. Robertson, *J. Chem. Soc., Dalton Trans.*, 1999, 1925.
19 O. Siri, G. Royal, A. Tabard, R. Guilard, V. Huch and M. Veith, *C. R. Acad. Sci., Sér. IIc: Chim.*, 1998, **1**, 557.
20 I. M. Helps, D. Parker, J. Chapman and G. Ferguson, *J. Chem. Soc., Chem. Commun.*, 1988, 1094.
21 J. Chapman, G. Ferguson, J. F. Gallagher, M. C. Jennings and D. Parker, *J. Chem. Soc., Dalton Trans.*, 1992, 345.
22 L. S. Hegedus and W. H. Moser, *J. Org. Chem.*, 1994, **59**, 7779.
23 D. A. Tomalia and L. R. Wilson, *US Pat.*, 4517122, 1985.
24 S. C. Dickerman and J. Simon, *J. Org. Chem.*, 1957, **22**, 259.
25 F. Denat, S. Brandès and R. Guilard, *Synlett*, 2000, 561.
26 A. E. Goeta, J. A. K. Howard, D. Maffeo, H. Puschmann, J. A. G. Williams and D. S. Yufit, *J. Chem. Soc., Dalton Trans.*, 2000, 1873.
27 F. Denat, S. Lacour, S. Brandès and R. Guilard, *Tetrahedron Lett.*, 1997, **38**, 4417.
28 H. Plenio and C. Aberle, *Chem. Commun.*, 1998, 2697.
29 T. J. Hubin, N. Tyryshkin, N. W. Alcock and D. H. Busch, *Acta Crystallogr., Sect. C*, 1999, **55**, 1888.
30 F. Rabiet, F. Denat and R. Guilard, *Synth. Commun.*, 1997, **27**, 979.
31 S. Brandès, F. Denat, S. Lacour, F. Rabiet, F. Barbette, P. Pullumbi and R. Guilard, *Eur. J. Org. Chem.*, 1998, 2349.
32 I. P. Beletskaya, G. A. Artamkina, V. A. Ivushkin and R. Guilard, *Tetrahedron Lett.*, 2000, **41**, 313.
33 K. Nakamoto, *Infrared and Raman Spectra of Inorganic and Coordination Compounds*, Wiley, New York, 1970.
34 R. M. Smith, A. E. Martell and R. J. Motekaitis, *NIST Critically Selected Stability Constants of Metal Complexes Database*, NIST Standard Reference Data No. 46, Gaithersburg, MD, 1997.
35 L. C. Siegfried and T. A. Kaden, *J. Phys. Org. Chem.*, 1992, **5**, 549.
36 B. Perlmutter–Hayman, *Acc. Chem. Res.*, 1986, **19**, 90.
37 R. M. Izatt, K. Pawlak, J. S. Bradshaw and R. L. Bruening, *Chem. Rev.*, 1991, **91**, 1721.
38 R. M. Izatt, K. Pawlak, J. S. Bradshaw and R. L. Bruening, *Chem. Rev.*, 1995, **95**, 2529.
39 P. G. Potvin and M. H. Wong, *Can. J. Chem.*, 1988, **66**, 2914.
40 J. Wiorkiewicz–Kuczera, K. Kuczera, C. Bazzicalupi, A. Bencini, B. Valtancoli, A. Bianchi and K. Bowman–James, *New J. Chem.*, 1999, **23**, 1007.
41 A. Bencini, A. Bianchi, E. Garcia–Espana, M. Micheloni and J. A. Ramirez, *Coord. Chem. Rev.*, 1999, **188**, 97.
42 A. M. Albrecht–Gary, S. Blanc, L. David and G. Jeminet, *Inorg. Chem.*, 1994, **33**, 518.
43 P. Caravan, T. Hedlund, S. Liu, S. Sjöberg and C. Orvig, *J. Am. Chem. Soc.*, 1995, **117**, 11230.
44 K. N. Raymond and J. M. McCormick, *J. Coord. Chem.*, 1998, **46**, 51.
45 L. J. Farrugia, *J. Appl. Crystallogr.*, 1997, **30**, 565.
46 J. Dale, *J. Chem. Soc.*, 1963, 93.
47 W. Klyne and V. Prelog, *Experientia*, 1960, **16**, 521.
48 J. Dale, *Acta Chem. Scand.*, 1973, **27**, 1115.
49 J. Dale, *Top. Stereochem.*, 1976, **9**, 199.
50 J. Dale, *Isr. J. Chem.*, 1980, **20**, 3.
51 W. N. Setzer, Y. P. Tang, G. J. Grant and D. G. Van Derveer, *Inorg. Chem.*, 1991, **30**, 3652.
52 M. Meyer, V. Dahaoui–Gindrey, C. Lecomte and R. Guilard, *Coord. Chem. Rev.*, 1998, **178–180**, 1313.
53 B. Bosnich, C. K. Poon and M. L. Tobe, *Inorg. Chem.*, 1965, **4**, 1102.
54 *International Tables for Crystallography*, ed. A. J. C. Wilson and E. Prince, Kluwer Academic Publishers, Dordrecht, 1999, vol. C.
55 E. Espinosa, E. Molins and C. Lecomte, *Chem. Phys. Lett.*, 1998, **285**, 170.
56 P. Gans, A. Sabatini and A. Vacca, *Talanta*, 1996, **43**, 1739.
57 X-RED 1.19, Stoe & Cie GmbH, Darmstadt, Germany, 1999.
58 Z. Otwinowski and W. Minor, *Methods Enzymol.*, 1997, **276**, 307.
59 G. M. Sheldrick, SHELXS-97, Program for the Solution of Crystal Structures, University of Göttingen, Göttingen, Germany, 1997.
60 G. M. Sheldrick, SHELXL-97, Program for the Refinement of Crystal Structures, University of Göttingen, Göttingen, Germany, 1997.